The International Journal of Advanced Manufacturing Technology (2018) 96:2943–2951
https://doi.org/10.1007/s00170-018-1810-7

ORIGINAL ARTICLE

Effects of drilling area temperature on drilling of carbon fiber reinforced polymer composites due to temperature-dependent properties

Hongxiao Wang [1] · Xiaohui Zhang [1] · Yugang Duan [1]

Received: 23 July 2017 / Accepted: 14 February 2018 / Published online: 26 February 2018

Abstract

The aim of this study was to investigate the influence of drilling area temperature on the material properties and quality of machined carbon fiber reinforced polymer (CFRP) composites. For this purpose, an epoxy resin matrix CFRP composite was chosen and tested under carefully designed temperature-controlled drilling experiments using a climatic chamber. The results show that the optimal range of drilling area temperatures is lower than the lower limit of the glass transition zone temperature (T_0) of the CFRP composite and higher than the upper limit for brittle deformation (T_b) of the resin. The reason for this is that when the drilling area temperature is higher than T_0, the interfacial shear strength (IFSS) and anti-deformation capacity of the CFRP composite are poor, which leads to surface roughness and a large amount of exit delamination damage. For drilling area temperatures lower than T_b, the CFRP becomes more brittle leading to a substantial increase in drilling thrust force, thereby increasing the probability of exit delamination damage. By solely maintaining the drilling area temperature between T_0 and T_b, the interlaminar fracture toughness, anti-deformation capacity, and IFSS of the composite can be increased, thereby decreasing the probability of drilling damage.

Keywords Composites machining · Temperature-dependent properties · Drilling area temperature · Interface properties · Ductile and brittle deformation

1 Introduction

Carbon fiber reinforced polymers (CFRPs) are widely used in the aerospace, automotive, and marine industries due to their high stiffness-to-weight and strength-to-weight ratios, high fatigue strength, and good corrosion performance [1]. However, CRFP composites are difficult to machine due to their inhomogeneous microstructure, anisotropy, high strength, and low thermal conductivity [2]. Drilling is a machining process frequently used in numerous industries for CFRP component assembly. However, machining-induced defects often occur during the drilling process and can seriously affect the performance of manufactured components. To minimize the damage caused by drilling, efforts have been made to decrease the drilling forces, including analyses of the tool shape [3–5], tool material [6–8], and machining process parameters [9, 10] used in conventional machining. While mechanical delamination is not the only factor that causes the damage during the machining of composite materials, temperature is another contributing factor. Due to the poor thermal conductivity of CFRPs, the drilling area temperature is always higher than the glass transition temperature (T_g) of the resin matrix [11, 12], and as a result, can lead to thermal damage [13].

To avoid thermal damage and improve drilling quality, the cryogenic machining method has been attempted in machining of fiber-reinforced composites and a number of advances have been made in this area in recent years. Bhattacharyya et al. [14] investigated the drilling of Kevlar fiber-reinforced composites under cryogenic conditions and reported improvements in the drilled hole surface quality and tool lifespan; however, under cryogenic conditions, the higher thrust force tends to increase the probability of delamination. Similarly, the effect of cryogenic cooling on drilling performance and the surface integrity of CFRP composite materials was explored by Xia et al. [15], and while cryogenic conditions were again found to enhance surface integrity, increased

✉ Yugang Duan
ygduan@xjtu.edu.cn

1 School of Mechanical Engineering, State Key Lab for Manufacturing Systems Engineering, Xi'an Jiaotong University, No. 99 Yangxiang Road, Xi'an, Shaanxi Province 710054, China

delamination also occurred due to the higher thrust force and torque. But, in both studies, the drilling temperature was not calibrated; in fact, the thrust force changed with temperature in a nonlinear way, and the delamination damage also changed with temperature. For example, in another study, Jia et al. examined the effect of different cooling temperatures on milling of CFRPs [16], the variation of cutting force with temperature was found to be nonlinear, and the quality of machined surface was also found changed with the temperatures due to the changes in the CFRP properties. However, the exact mechanism leading to the temperature-dependent effects on the quality of drilled holes, moreover, how to determine the optimal drilling temperature, still remain unclear.

Herein, we study the influence of temperature on the material properties and quality of machined CFRPs and propose a method to control the drilling area temperature, thereby improving the quality of drilled holes. Static tensile testing of the resin, microdroplet debonding tests, and double cantilever beam (DCB) tests were performed to study the temperature-dependent properties of the resin, interfacial shear strength (IFSS), and fracture toughness of the CFRP, respectively.

2 Experimental procedure

2.1 Preparation of CFRP specimens

The CFRP composite used in this study was a carbon T300/epoxy unidirectional prepreg with a ply thickness of 0.125 mm, purchased from Hengshen Co. Ltd., China. The stacking sequence of the carbon/epoxy laminates was $[45/0/-45/90]_{6s}$ (totally 48 plies) with a total thickness of 6 ± 0.2 mm, and each specimen was 150 × 100 mm. The mechanical properties of the T300/epoxy composite are provided in Table 1.

2.2 Dynamic mechanical analysis of CFRP

To study the anti-bending performance and anti-deformation capacity of the CFRP at different temperatures and to measure the T_g, dynamic mechanical analysis (DMA) tests were conducted with three-point bending modes, according to *ASTM D5023-15*. Test specimens of the CFRP were prepared with dimensions of 60 × 13 × 3 mm, and temperature scanning measurements were performed across an ambient temperature range of 0 to 150 °C, at a heating rate of 3 °C/min and oscillation frequency of 1 Hz.

2.3 Microdroplet debonding method for measuring interfacial shear strength

The IFSS is an important property of CFRP composites, which influences adhesion between the fibers and matrix [17, 18]. The microdroplet debonding method was used to assess the dependence of IFSS on temperature [19]. Temperatures ranging from 23 to 120 °C (at 30 °C increments) were tested. A total of five tests were performed at each temperature. Carbon fibers with a 7-μm diameter were embedded in epoxy resin microdroplets and maintained at an embedded length of 70–90 μm and a contact angle of 40°–45°. The force required to pull the carbon fiber out of the cured epoxy resin was measured using a microdroplet test machine (HM410; Tohei Sangyo, Japan). For each specimen, the IFSS, denoted τ_{IFSS}, was estimated using the following equation [19]:

$$\tau_{IFSS} = \frac{F_{\max}}{\pi \times d_f \times l_e} \tag{1}$$

where $F_{\max}$ is the maximum value of the pullout force (N), d_f is the diameter of a single fiber (mm), and l_e is the embedded length of the microdroplet (mm).

Table 1 Mechanical properties of T300/epoxy composite at room temperature

Elastic properties	CFRP
Longitudinal stiffness, E_{11} (MPa)	137,000
Transverse stiffness, E_{22} (MPa)	9000
Poisson's ratio, υ_{12}	0.28
Shear moduli, G_{12} (MPa)	6000
Fiber content (%)	60 ± 2

2.4 Tensile testing of epoxy resin

The temperature-dependent properties of the resin were determined under tensile loading using a universal testing machine (CMT4304; MTS, USA), according to *ASTM D638-10* "*Standard Test Method for Tensile Properties of Plastics.*" The dumbbell-shaped specimens (type I) were stretched using an extensometer at a rate of 2 mm/min, and the stress-strain curves were recorded for ambient temperatures ranging from 23 to 120 °C (at 30 °C increments) in a climatic chamber. For each condition, five tests were performed.

2.5 Double cantilever beam test to measure the mode I interlaminar fracture toughness

Fracture toughness is a key parameter of CFRPs since it influences the critical thrust force of drilling, which can lead to delamination [20]; therefore, it is important to study the temperature dependence of the mode I interlaminar fracture toughness (G_{IC}). The influence of temperature on G_{IC} was tested using the double cantilever beam (DCB) test, according to *ASTM D5528-01*. The sample dimensions were 140 × 25 × 3.5 mm, and the initial delamination length was 50 mm. All tests were performed at a speed of 1 mm/min, using the same temperature range of 23 to 120 °C (at 30 °C increments). Five

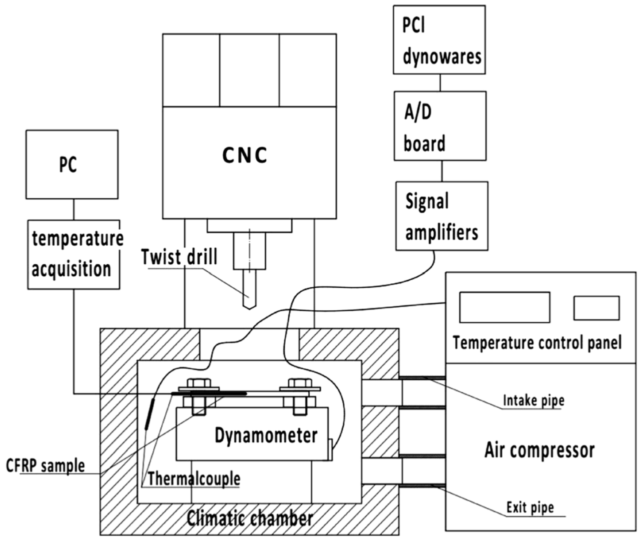

Fig. 1 Schematic of temperature-controlled drilling experiment setup including the force and temperature measurement instruments

tests were performed for at each temperature. The following equation was used to calculate G_{IC} [21]:

$$G_{IC} = \frac{3P\delta}{2ba} \qquad (2)$$

where P is the load (N), δ is the load point displacement (mm), b is the specimen width (mm), and a is the delamination length (mm).

2.6 Setup of temperature-controlled drilling experiments

Temperature-controlled drilling tests were carried out using a cooling drilling system (Fig. 1). The system was composed of a vertical drilling-milling machine, climatic chamber, cryogenic cooling device, temperature measurement gauge, and drill force measurement device. Specimens were placed in the chamber and secured by a steel support and clamp (Fig. 1). Thermocouple sensors were used to measure the ambient temperature inside the climatic chamber and local drilling area temperature. The temperature was regulated by an electrovalve, which controls the volume of cold air entering the chamber. The cutting forces under different drilling temperatures were collected via a Kistler data acquisition system (5697A) consisting of a dynamometer (9253B) and amplifier (5080). For all drilling experiments, a vertical drilling-milling machine with a maximum spindle speed of 3000 rpm was used with several different uncoated carbide conventional twist drills (diameter 8 mm, point angle 118°).

Four ambient temperature conditions were considered, − 50, − 25, 0, and 23 °C, and a fresh drill was used for each test. The drilling area temperature is influenced by the cutting speed, feed rate, drill material, and drill geometry in a very complex way; therefore, single-factor experiments were conducted to determine the variation of drilling quality with temperature. The cutting speed was held constant at 1000 r/min with a linear feed of 20 mm/min. Five specimens were tested at each temperature.

3 Results and discussion

3.1 Effect of temperature on material properties of CFRP-epoxy resin composites

The thermal damage that occurs during drilling is caused by higher drilling temperatures, due to the thermal instability of resin matrix composites; thus, it is important to study the effect of temperature on the material properties. The storage

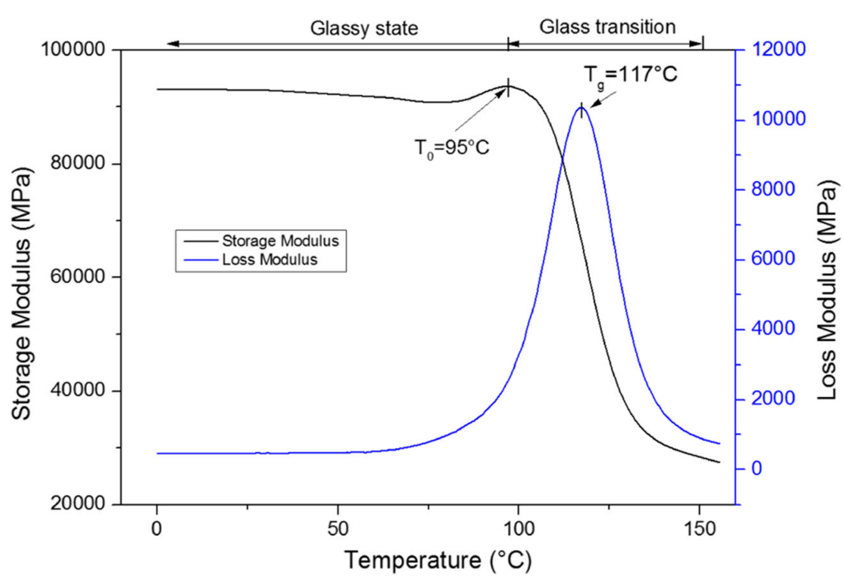

Fig. 2 Representative curves of the storage modulus (left axis) and loss modulus (right axis) versus temperature for a carbon/epoxy resin composite measured by DMA. The glassy region and glass transition region are shown

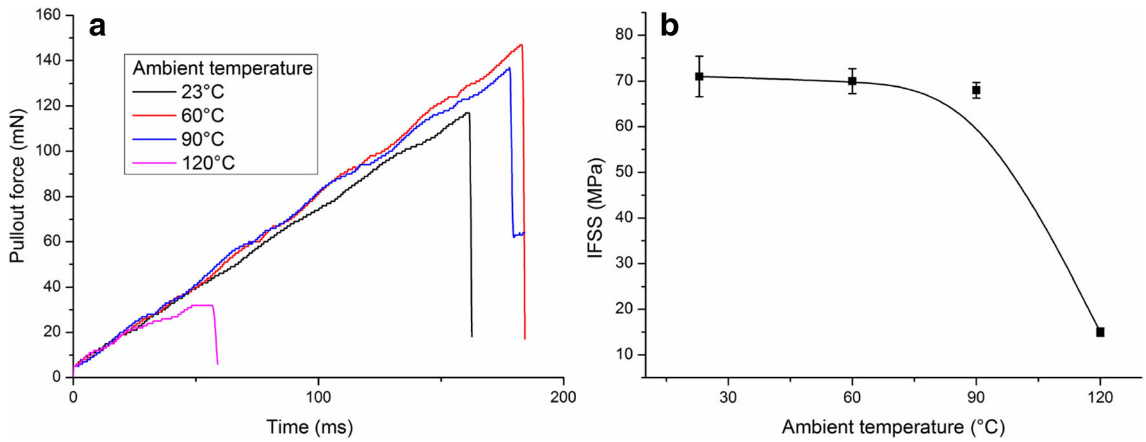

Fig. 3 Results of the microdroplet debonding tests. **a** Representative curves of the pullout force versus time for different drilling temperatures. **b** Graph of IFSS versus ambient temperature. Error bars represent ± one standard deviation

modulus is commonly used to characterize the anti-deformation capacity of materials, and a higher storage modulus indicates a material with a greater anti-deformation capacity, which is advantageous in machining. Figure 2 shows the storage modulus and loss modulus versus temperature of the CFRP measured using DMA with three-point bending modes. The IFSS is always used to characterize the adhesion between the fibers and matrix, and a higher IFSS is better to improve the drilled surface quality. Representative curves of the pullout force versus temperature and the graph of IFSS versus ambient temperature are shown in Fig. 3a, b. From Figs. 2 and 3, it can clearly be observed that the storage modulus and IFSS are significantly affected by temperature. For a temperature range of 23 to 95 °C, the resin is in a glassy state (Fig. 2), and the storage modulus and IFSS remain relatively steady (Fig. 3b), which improves the quality of drilled holes. Within the temperature ranges of 95 to 120 °C, the resin is in the glass transition state (Fig. 2), and the storage modulus and IFSS decline sharply (Fig. 3b), which is unfavorable for the machining process. The lower limit of the glass transition state, denoted T_0, is 95 °C (Fig. 2).

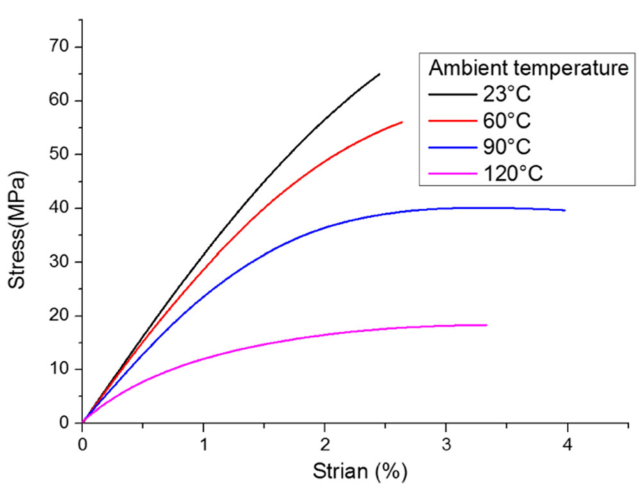

Fig. 4 Representative stress-strain curves of the epoxy resin under different temperatures

Although the storage modulus and IFSS of the composite in the glassy state remain stable, this does not mean that the entire temperature range within the glassy state is suitable for machining, since there is variation within this temperature in the matrix toughness and G_{IC}—also important factors that influence drilling quality. Stress-strain curves of the epoxy resin under different temperatures are shown in Fig. 4. The corresponding micromorphologies of fractured sections following tensile testing were observed under an optical microscope (VH-8000, Keyence, Japan), as shown in Fig. 5a–d. From Figs. 4 and 5, it can be observed that the epoxy resin becomes less brittle as the ambient temperature increases and toughness increases; moreover, the critical temperature between toughness and brittleness is approximately 60 °C (T_b). Along with the DMA curves for the CFRP, two deformation modes can be identified in the glassy state—the ductile deformation zone (60 °C < T < 95 °C) and brittle deformation zone (T < 60 °C), which influence the material removal mechanism and thus influences drilling quality.

In contrast to the material properties described above, G_{IC} is the main factor that influences the exit delamination of the drilled CFRP. Previous studies have shown that the critical thrust force for delamination is related to G_{IC} [22], and increasing the value of G_{IC} can improve the critical axial force and thus reduce the probability of delamination. However, the fracture toughness of the CFRP also changes with temperature. Representative force-displacement curves of the double cantilever beam test for different ambient temperatures are shown in Fig. 6a, and the graphs of G_{IC} versus temperature are presented in Fig. 6b. G_{IC} increases with temperature, exponentially so within the range of 90 to 120 °C. However, unrecovered deformation (Fig. 6a), which influences drilling quality, also occurs in the glass transition temperature range, defined as temperatures higher than T_0, due to the lower storage modulus. The effects of temperature on the material

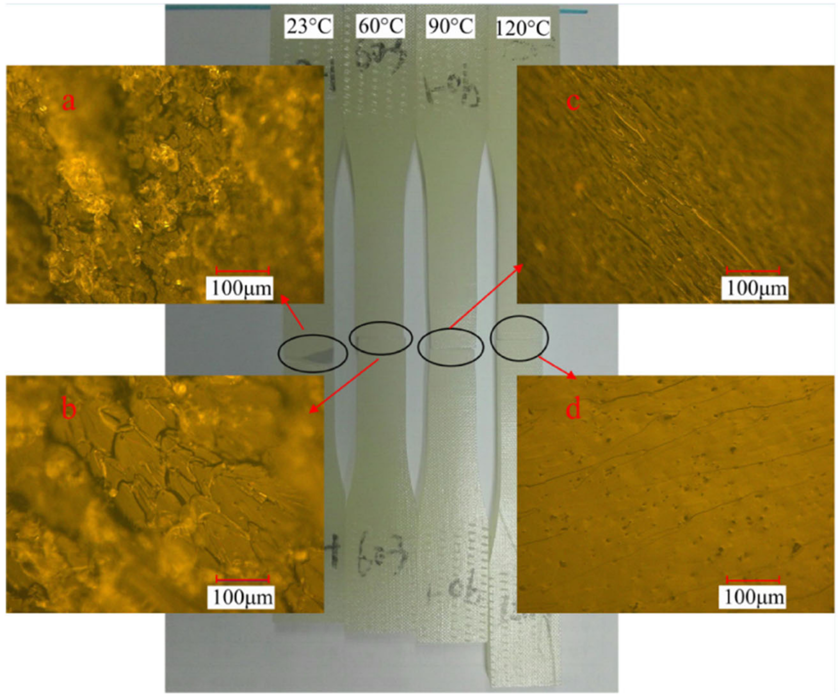

Fig. 5 Representative images of the morphologies of fractured cross sections after tensile testing under different temperatures. **a** 23 °C. **b** 60 °C. **c** 90 °C. **d** 120 °C

properties are summarized in Table 2. Based on the dependence of the material properties on temperature within the different temperature ranges, the drilling quality of the CFRP will also change with temperature.

3.2 Influence of drilling area temperature on the quality of the drilled surface

The drilling ambient temperature refers to the air temperature within the climatic chamber, which differs from the local drilling area temperature. The temperature-dependent properties of the material within the local drilling area change with the drilling area temperature. For each ambient temperature, representative curves of the drilling area temperature versus time are shown in Fig. 7, and the maximum temperature of each test is the real-time temperature between the tool and specimen engagement area, called the drilling area temperature. Before drilling, the initial ambient temperatures were controlled at approximately 23, 0, − 25, or − 50 °C. During drilling, the corresponding drilling area temperatures were measured as approximately 128, 100, 73, or 45 °C, respectively (Fig. 7).

The evolution of surface roughness (Ra) as a function of drilling area temperature was measured using a confocal laser scanning microscope (OLS4000, Olympus, Japan), as illustrated in Fig. 8. The drilling area temperature was shown to significantly influence Ra along both the parallel and perpendicular hole axis directions. At 73 °C (ambient temperature of

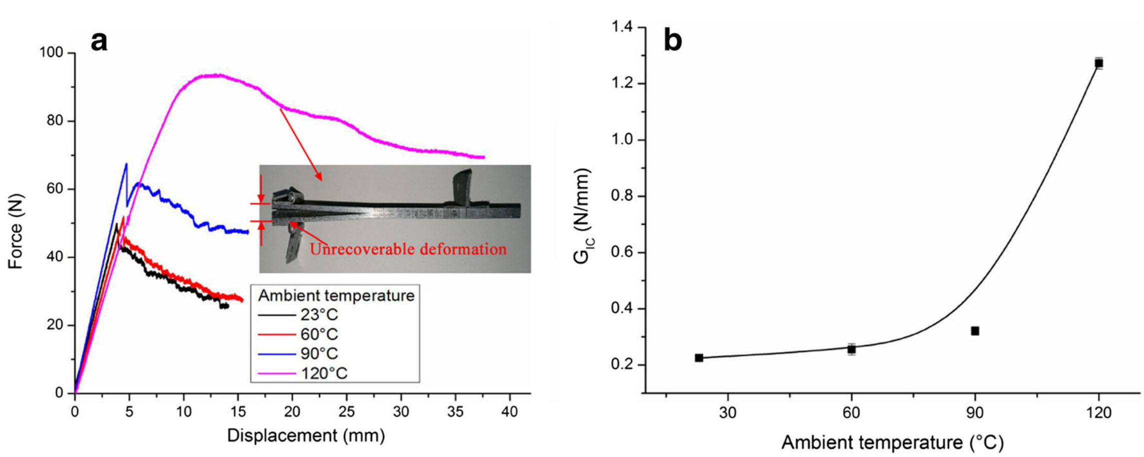

Fig. 6 Results of DCB testing. **a** Representative force-displacement curves for each ambient temperature. The image inlay shows the extent of unrecoverable damage caused at the highest temperature. **b** Graph of G_{IC} versus ambient temperature

Table 2 Effects of temperature on material properties

Experiment	Material properties	Glassy state		Glass transition state
		23 °C < T < 60 °C	60 °C < T < 95 °C	95 °C < T
DMA test	Storage modulus	Remains stable	Remains stable	Decreases sharply
Microdroplet debonding test	IFSS	Remains stable	Remains stable	Decreases sharply
Resin tensile testing	Toughness	Increases	Increases	Increases
	Failure mode	Brittle failure	Ductile failure	Ductile failure
Double cantilever beam test	G_{IC}	Increases	Increases	Increases exponentially

− 25 °C), the Ra values reaches the lowest point, reduced by 51.9 and 53.8% along the parallel and perpendicular hole axis directions, respectively, compared to 128 °C (ambient temperature of 23 °C). The relationship between Ra and drilling area temperature does not appear to be linear, as the Ra values increase from 73 to 45 °C trend to be stable. To further investigate the mechanism behind changes in the drilled hole surface roughness with drilling area temperature, micromorphologies of the drilled surface were observed using a scanning electron microscope (SEM, su-8010, Hitachi, Japan), and analyzed.

The cross-sectional micromorphologies of the drilled surfaces for various drilling area temperatures are presented in Fig. 9 (a–d), and higher magnification images are shown in Fig. 9 (a1–d1). It can be observed that the material removal mechanism changes depending on temperature (Fig. 9). Areas showing differing amounts of residual resin material (Fig. 9 (a1–d1)) demonstrate the relationship between drilled surface quality and drilling area temperature. The amount of drilling area resin is related to the temperature-dependent properties of the interface, which highlights the importance of researching the temperature-dependent properties of the resin and drill-material interface under a range of drilling area temperatures.

For the range of drilling area temperatures greater than T_0, the resin is in the glass transition state and the IFSS declines sharply. Consequently, there are more defects on the drilled surfaces within this temperature range (Fig. 9 (a and b, a1 and b1)), due to the lower IFSS values, which leads to a large amount of resin being taken away by the drill during the process. When the temperature ranges from 23 °C to T_0, the resin is in the glassy state and the IFSS remains relatively steady. Therefore, the interface is enhanced and can be characterized by changes in the material removal mechanism, a large amount of resin on the surface of the composite results in an optimal surface for drilling (Fig. 9 (c and d, c1 and d1)). However, due to the variation in toughness of the resin matrix, the material removal mechanism will also change within this temperature range. When the drilling area temperature is held constant at approximately 73 °C, the resin in the drilling area undergoes ductile deformation and failure, resulting in a smoother drilled surface. In contrast, when the drilling area temperature is approximately 45 °C, the resin in the drilling area undergoes brittle deformation and the material removal mechanism changes to brittle fracture, ultimately leading to surface a small amount of roughness (Fig. 9 (d, d1)). Thus, maintaining the drilling area temperature to be within the

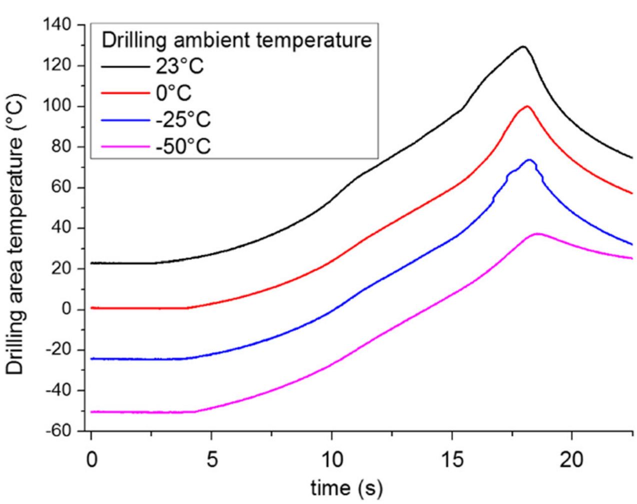

Fig. 7 Changes in the drilling area temperature over the total drilling time. Representative curves of the drilling area temperature versus time for each ambient temperature within the climatic chamber

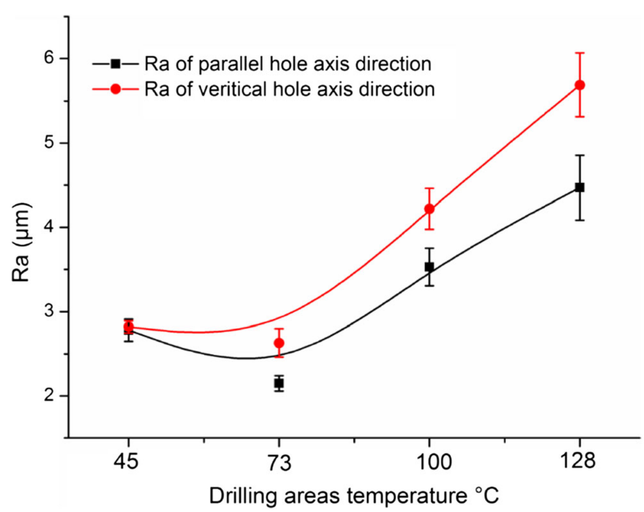

Fig. 8 Influence of drilling area temperature on Ra. Graph of Ra versus drilling area temperature in the parallel and perpendicular hole axis directions. Error bars represent ± one standard deviation

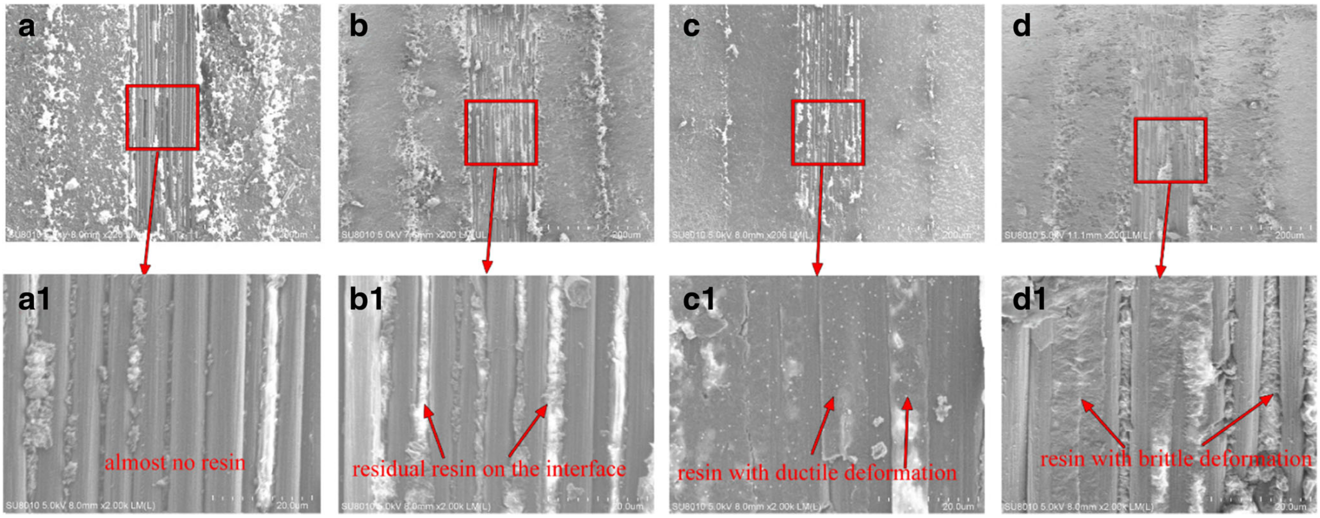

Fig. 9 SEM micrographs of the cross sections of the drilled surfaces for various drilling area temperatures: 128 °C (a and a1), 100 °C (b and b1), 73 °C (c and c1), and 45 °C (d and d1). Arrows indicate the presence of resin on the drilling surface

lower temperature range is an effective method for decreasing the Ra value; however, reducing the temperature too much may reduce this effect. By controlling the drilling area temperature to below T_0 and higher than T_b, it is possible to reduce surface roughness, and thereby improve the quality of the drilled surface.

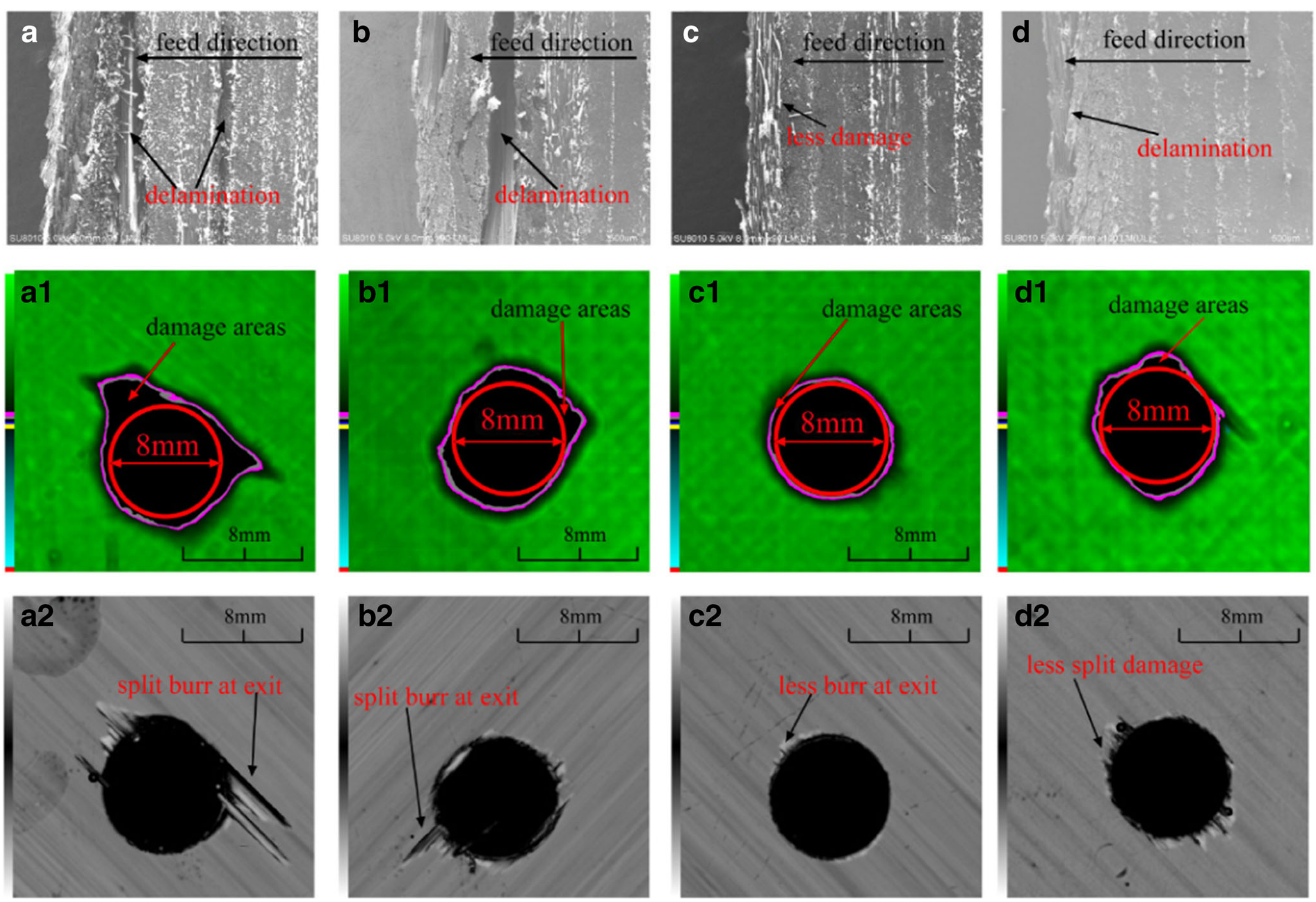

Fig. 10 Exit damage under various drilling area temperatures: 128 °C (a and a1), 100 °C (b and b1), 73 °C (c and c1), and 45 °C (d and d1). Representative SEM images of the wall surface within a drilled hole (a–d). Arrows indicate delamination damage and feed direction. Ultrasonic C-scans of delamination damage, indicated by red arrows (a1–d1). Ultrasonic C-scans of damage at the exit surface, indicated by red arrows (a2–d2)

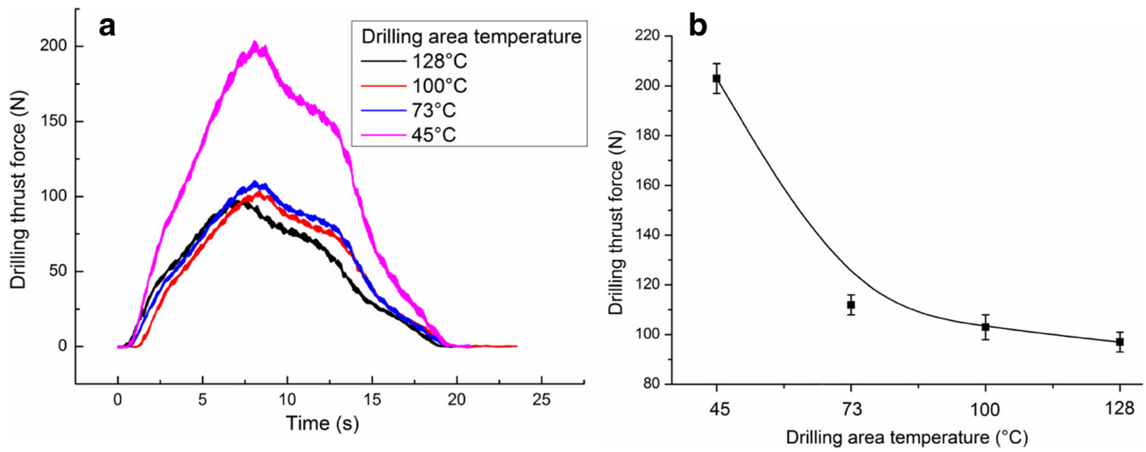

Fig. 11 Graphs of drilling thrust force versus drilling area temperature. **a** Representative curves of the drilling thrust force versus time for different drilling area temperatures. **b** Influence of the drilling area temperature on the maximum drilling force. Graph of drilling thrust force versus drilling area temperature. Error bars represent ± one standard deviation

3.3 Influence of drilling area temperature on exit damage

Exit-ply delamination can be a serious issue during the drilling process [23–25]. To observe the extent of exit damage caused by the drill at different temperatures, SEM was performed, and ultrasonic C-scans were taken using an acoustic microscope (D9500, Sonoscan, USA). Representative SEM images of the inner walls of each drilled hole are shown in Fig. 10 (a–d). Delamination damage and exit surface damage can be observed in the ultrasonic C-scan images, as shown in Fig. 10 (a1–d1 and a2–d2, respectively). From Fig. 10, it is clear that the amount delamination damage varies with the drilling area temperature. When the drilling area temperature is higher than T_0, serious delamination damage occurs in the exit-ply (Fig. 10 (a and b, a1 and b1, a2 and b2)). For drilling area temperatures lower than T_0, within the ductile deformation temperature range, less delamination is observed (Fig. 10 (c1)) and the exit surface shows little or no damage (Fig. 10 (c, c2)). However, at the lowest drilling area temperature (45 °C), the material enters the brittle deformation zone, and the damage due to delamination becomes worse (Fig. 10 (d, d1)), despite less damage due to splitting of the exit surface (Fig. 10 (d2)).

Previous studies have shown that exit delamination during the drilling of CFRPs is related to the critical thrust force and the drilling thrust force. If the drilling thrust force is greater than the critical value, delamination damage occurs. A higher G_{IC}indicates a higher critical thrust force, and from Fig. 6b, it can be observed that G_{IC}increases exponentially for temperatures higher than T_0; however, the delamination damage is more evident in this temperature range (Fig. 10 (a and b)). On one hand, the lower IFSS in this temperature range causes split burrs at the exit and worsens the exit delamination damage (Fig. 10 (a2 and b2)). On the other hand, the DMA results show that the anti-bending properties and anti-deformation capacity of CFRP decrease sharply in this temperature range (Fig. 2). For this reason, serious delamination damage occurs at the exit when the drilling area temperature is greater than T_0 (Fig. 10 (a1 and b1)). Nonetheless, this does not suggest that all drilling area temperatures lower than T_0 can avoid delamination damage since the drilling thrust force will also change with the drilling area temperature.

The general relationship between the drilling thrust force and drilling area temperature is shown in Fig. 11a, b. As the drilling area temperature decreases, the drilling thrust force increases exponentially. Whereas only small incremental changes in the drilling thrust force are observed from 97 to 112 N with a corresponding decrease in the drilling area temperature from 128 to 73 °C, a sharp increase to 203 N was observed following a drop in drilling area temperature from 73 to 45 °C. This suggests that drilling in the brittle deformation zone results in a substantial increase in the drilling thrust force, thereby increasing the probability of exit delamination damage. Thus, considering the results of both the drilling thrust force versus temperature and the temperature dependence of G_{IC} and IFSS, excessively high or low drilling area temperatures increase the probability of drilling delamination damage of the CFRP. Therefore, to avoid drilling delamination damage, the optimal drilling area temperature should be lower than T_0 and higher than T_b.

4 Conclusions

In this study, the influence of ambient temperature on the machining quality of a CFRP-epoxy resin composite was experimentally assessed and a drilling area temperature control method was proposed to improve the quality of drilled holes.

The following conclusions can be drawn:

1. The material removal mechanism varies with drilling area temperature due to a number of temperature-dependent properties, including IFSS and resin toughness. For drilling area temperatures higher than T_0, IFSS sharply decreases leading to large defects in the drilled hole surface. Conversely, drilling area temperatures lower than T_0, and which are maintained within the ductile deformation zone of the resin, can enhance the interface and resin toughness, resulting in a more smoother drilled surface. Lastly, for drilling area temperatures lower than T_b, the material removal mechanism changes from ductile to brittle fracture leading to a small increase in Ra.
2. The exit delamination damage improves with different drilling area temperatures since the IFSS, G_{IC}, and drilling thrust force also change. Drilling area temperatures higher than T_0 result in poor IFSS, as well as poor anti-bending properties and anti-deformation capacity, and therefore lead to greater exit damage. The increase in brittleness of the CFRP is a result of lower drilling area temperatures and leads to a significant increase in the drilling thrust force, thereby increasing the probability of exit delamination damage. Controlling the drilling area temperature below T_0 within the ductile deformation zone can increase its fracture toughness and the IFSS, thereby decreasing the probability of exit delamination damage.
3. Drilling area temperatures that are excessively high or low are of no benefit to the drilling quality of CFRP composites; therefore, a suitable temperature range for drilling epoxy resin composites is one that is lower than T_0 and higher than T_b, which can be determined by DMA and tensile testing.

Funding information The authors gratefully acknowledge financial support from the Fundamental Research Funds for the Central Universities (grant no. xjj201760).

References

1. Iliescu D, Gehin D, Iordanoff I, Girot F, Gutiérrez ME (2010) A discrete element method for the simulation of CFRP cutting. Compos Sci Technol 70(1):73–80
2. Shokrani A, Dhokia V, Newman ST (2012) Environmentally conscious machining of difficult-to-machine materials with regard to cutting fluids. Int J Mach Tool Manu 57(2):83–101
3. Tsao CC (2006) The effect of pilot hole on delamination when core drill drilling composite materials. Int J Mach Tool Manu 46(12–13):1653–1661
4. Tsao CC, Chiu YC (2011) Evaluation of drilling parameters on thrust force in drilling carbon fiber reinforced plastic (CFRP) composite laminates using compound core-special drills. Int J Mach Tool Manu 51(9):740–744
5. Tsao CC, Hocheng H (2008) Analysis of delamination in drilling composite materials by core-saw drill. Int J Mater Prod Technol 32(2–3):188–201
6. Mkaddem A, Soussia AB, Mansori ME (2013) Wear resistance of CVD and PVD multilayer coatings when dry cutting fiber reinforced polymers (FRP). Wear 302(1–2):946–954
7. Faraz A, Biermann D, Weinert K (2009) Cutting edge rounding: an innovative tool wear criterion in drilling CFRP composite laminates. Int J Mach Tool Manu 49(15):1185–1196
8. Karpat Y, Değer B, Bahtiyar O (2014) Experimental evaluation of polycrystalline diamond tool geometries while drilling carbon fiber-reinforced plastics. Int J Adv Manuf Technol 71(5–8):1295–1307
9. Phadnis VA, Makhdum F, Roy A, Silberschmidt VV (2013) Drilling in carbon/epoxy composites: experimental investigations and finite element implementation. Compos A: Appl Sci Manuf 47(1):41–51
10. Rao GVG, Mahajan P, Bhatnagar N (2007) Micro-mechanical modeling of machining of FRP composites—cutting force analysis. Compos Sci Technol 67(3–4):579–593
11. Weinert K, Kempmann C (2004) Cutting temperatures and their effects on the machining behaviour in drilling reinforced plastic composites. Adv Eng Mater 6(8):684–689
12. Yashiro T, Ogawa T, Sasahara H (2013) Temperature measurement of cutting tool and machined surface layer in milling of CFRP. Int J Mach Tool Manu 70(4):63–69
13. Santiuste C, Diaz-Alvarez J, Soldani X, Miguelez H (2013) Modelling thermal effects in machining of carbon fiber reinforced polymer composites. J Reinf Plast Compos 33(8):758–766
14. Bhattacharyya D, Horrigan DPW (1998) A study of hole drilling in Kevlar composites. Compos Sci Technol 58(2):267–283
15. Xia T, Kaynak Y, Arvin C, Jawahir IS (2016) Cryogenic cooling-induced process performance and surface integrity in drilling CFRP composite material. Int J Adv Manuf Technol 82(1):605–616
16. Jia Z, Fu R, Wang F, Qian B, He C (2016) Temperature effects in end milling carbon fiber reinforced polymer composites. Polym Compos 39:437–447
17. Miller B, Muri P, Rebenfeld L (1987) A microbond method for determination of the shear strength of a fiber/resin interface. Compos Sci Technol 28(1):17–32
18. Pitkethly MJ, Favre JP, Gaur U, Jakubowski J, Mudrich SF, Caldwell DL, Drzal LT, Nardin M, Wagner HD, di Landro L, Hampe A, Armistead JP, Desaeger M, Verpoest I (1993) A round-robin programme on interfacial test methods. Compos Sci Technol 48(1–4):205–214
19. Yang L, Thomason JL (2010) Interface strength in glass fibre–polypropylene measured using the fibre pull-out and microbond methods. Compos A: Appl Sci Manuf 41(9):1077–1083
20. Liu C, Wang G, Ren C, Yang Y (2014) Mechanistic modeling of oblique cutting considering fracture toughness and thermo-mechanical properties. Int J Adv Manuf Technol 74(9–12):1459–1468
21. O'Brien TK, Martin RH (1993) Round Robin testing for mode I interlaminar fracture toughness of composite materials. J Compos Technol Res 15(4):269–281
22. Gururaja S, Ramulu M (2009) Modified exit-ply delamination model for drilling FRPs. J Compos Mater 43(5):483–500
23. Haddad M, Zitoune R, Eyma F, Castanie B (2014) Study of the surface defects and dust generated during trimming of CFRP: influence of tool geometry, machining parameters and cutting speed range. Compos A: Appl Sci Manuf 66(6):142–154
24. Haddad M, Zitoune R, Eyma F, Castanié B (2015) Influence of machining process and machining induced surface roughness on mechanical properties of continuous fiber composites. Exp Mech 55(3):519–528
25. Saleem M, Toubal L, Zitoune R, Bougherara H (2013) Investigating the effect of machining processes on the mechanical behavior of composite plates with circular holes. Compos A: Appl Sci Manuf 55(6):169–177